ORIGINAL RESEARCH

Improving antitumor outcomes for palliative intratumoral injection therapy through lecithin–chitosan nanoparticles loading paclitaxel–cholesterol complex

Xiao-Yang Chu,[1–3,]* Wei Huang,[2,]* Yu-Li Wang,[1] Ling-Wei Meng,[2] Li-Qing Chen,[2] Ming-Ji Jin,[2] Lu Chen,[1] Chun-Hong Gao,[1] Cheng Ge,[3] Zhong-Gao Gao,[2] Chun-Sheng Gao[1]

[1]State Key Laboratory of Toxicology and Medical Countermeasures, Beijing Institute of Pharmacology and Toxicology, Beijing 100850, P.R. China; [2]State Key Laboratory of Bioactive Substance and Function of Natural Medicines, Department of Pharmaceutics, Institute of Materia Medica, Chinese Academy of Medical Sciences and Peking Union Medical College, Beijing 100050, P.R. China; [3]Department of Stomatology, The 5th Medical Center of Chinese PLA General Hospital, Beijing 100071, P.R. China

*These authors contributed equally to this work

Correspondence: Chun-Sheng Gao
State key Laboratory of Toxicology and Medical Countermeasures, Beijing Institute of Pharmacology and Toxicology, 27 Tai Ping Road, Beijing 100850, P.R. China
Email gaocs@bmi.ac.cn

Zhong-Gao Gao
State Key Laboratory of Bioactive Substance and Function of Natural Medicines, Institute of Materia Medica, Chinese Academy of Medical Sciences and Peking Union Medical College, 1 Xian Nong Tan Street, Beijing 100050, P.R. China
Email zggao@imm.ac.cn

Background: Intratumoral injection is a palliative treatment that aims at further improvement in the survival and quality of life of patients with advanced or recurrent carcinomas, or cancer patients with severe comorbidities or those with a poor performance status.

Methods: In this study, a solvent-injection method was used to prepare paclitaxel–cholesterol complex-loaded lecithin–chitosan nanoparticles (PTX-CH-loaded LCS_NPs) for intratumoral injection therapy, and the physicochemical properties of NPs were well characterized.

Results: The particle size and zeta potential of PTX-CH-loaded LCS_NPs were 142.83±0.25 nm and 13.50±0.20 mV, respectively. Release behavior of PTX from PTX-CH-loaded LCS_NPs showed a pH-sensitive pattern. The result of cell uptake assay showed that PTX-CH-loaded LCS_NPs could effectively enter cells via the energy-dependent caveolae-mediated endocytosis and macropinocytosis in company with the Golgi apparatus. Meanwhile, PTX-CH-loaded LCS_NPs had a better ability to induce cell apoptosis than PTX solution. The in vivo antitumor results suggested that PTX-CH-loaded LCS_NPs effectively inhibited mouse mammary cancer growth and metastasis to distant organs and significantly improved the survival rate of tumor-bearing mice by intratumoral administration.

Conclusion: In general, our study demonstrated that PTX-CH-loaded LCS_NPs used for palliative treatment by intratumoral injection showed improved safety and antitumor efficacy, which provided an alternative approach in the field of palliative chemotherapy.

Keywords: lecithin, chitosan, paclitaxel, nanoparticles, pH responsive, palliative chemotherapy, intratumoral injection

Introduction

For early stage malignant solid tumors, the preferred treatment is surgical resection, unless adjacent important structures prevent complete excision. But for advanced carcinomas at stage III–IV or inoperable sites, surgical excision is not an effective treatment, which necessitates new treatment modalities for some esophageal carcinomas,[1] lung cancers,[2] and gastrointestinal cancers,[3,4] as reported. And for patients with severe comorbidities or a poor performance status, such as the elderly patients, they cannot undergo the injury caused by surgical treatment. Treatment of inoperable and metastatic disease requires a systemic treatment strategy. To get further improvements in survival and quality of life, two options for palliative treatment remain: palliative irradiation and chemotherapy.[5] Radiation therapy may be an option to unresectable tumors of certain histologic types, but for the radiation-insensitive tumors, we have to turn to chemotherapy. The dose of a chemotherapeutic agent used for systemic

chemotherapy delivered systemically might be toxic on vital organs and tissues, which requires a good performance status of the patients. As for inoperable radiation-insensitive cancer patients with a poor performance status, palliative intratumoral injection chemotherapy may provide a meaningful response.

Palliative intratumoral injection chemotherapy is clinically used in treating lung cancer guided with bronchoscopic endobronchial ultrasound,[6,7] central airway obstruction caused by lung carcinoma,[8] extremity melanoma,[9] dysphagia caused by carcinoma,[10] malignant biliary obstruction,[11] recurrent head and neck squamous cell carcinoma,[5,12,13] and midcervical carcinoma.[14] In recent years, several intratumoral delivery systems have been developed that are mainly based on polymers and involve hydrogels,[15–18] microparticles,[13,19] nanoparticles,[20] nanofibers,[21] etc. For intratumoral injection formulation, hydrogels were publicly recognized, including modified chitosan thermosensitive hydrogel[17,18] and poly (ε-caprolactone) nanoparticles amalgamated with in situ gel.[16] For localized therapy, intratumoral injection leads to a long retention time at the site that consequently releases the antitumor drug in a continuous and sustained manner. And the nanoparticles need more efficient drug delivery into cancer cells to achieve the enhanced permeation and retention (EPR) effect.[22] However, the gels were mostly thermosensitive or pH sensitive, and they would turn into solid once injected into tumor so that the drug was distributed inside the solid tumor unevenly and pressure problems followed. Lecithin–chitosan nanoparticles, as a carrier of hydrophobic drugs, were positively charged as reported and, might be strongly attached to the negatively charged cell membrane, which could enhance the EPR effect of nanoparticles at tumor sites and offer better coverage for topical drug delivery,[23–25] ultimately exerting quick efficacy in the tumor. The extracellular pH of solid tumors and lysosome is lower than that of normal tissues.[26] The release of drugs loaded in chitosan nanoparticles could be accelerated by decreasing the media pH.[15] The pH sensitivity behavior could accelerate drug release at tumor sites and decrease the side effects, which can contribute to the targeted tumor treatment.

Chitosan, as an important component of lecithin–chitosan nanoparticles, is a natural cationic amino polysaccharide polymer. Chitosan and its derivatives have been widely used in drug delivery systems thanks to their biocompatibility, nontoxicity, a high encapsulation rate, controllable drug release, and target property to specific tissues.[27,28] Chitosan can form self-assembled nanoparticles with negatively charged materials, such as lecithin, which is considered to be an important characteristic for the preparation of drug-loaded

microemulsions, liposomes, micelles, and nanoparticles.[24,25] The ideal chitosan nanoparticles should be positively charged and tumor targeting with sustained and pH-sensitive drug release.

Paclitaxel (PTX) is a significant antitumor chemotherapy drug in clinical treatments against multiple solid tumors, especially against metastatic breast cancer, small and non-small-cell lung cancer, colon cancer, ovarian cancer, and head and neck cancer,[29,30] by intervening with the normal breakdown of microtubules during cell division. In clinical, the formulation of PTX is called Taxol®, which is mixed with Cremophor EL and dehydrated ethanol to solve the problem of poor water solubility. But the formulation can induce severe side effects if administered by intravenous injection, such as allergic reactions, renal toxicity, neurotoxicity, hypersensitivity, and dyspnea in patients.[31] Researchers have been working hard to solve poor solubility and nonspecific biodistribution. Abraxane®, a formulation of albumin–PTX nanoparticles approved by FDA in 2006, was reported to be able to improve the antitumor efficacy, but there was no improvement in pharmacokinetic properties compared with Taxol, because of poor colloidal stability of Abraxane.[32] Therefore, the formulation of ideal PTX nanoparticles should be characterized by nontoxicity, high encapsulate rates, controllable drug release, target property to tumor tissue, and stability during blood circulation, all of which lecithin–chitosan nanoparticles can achieve. PTX as a lipophilic drug can be incorporated into the interior lecithin layers of lecithin–chitosan nanoparticles, but PTX does not have sufficiently high solubility in lecithin. The solubility of PTX in lecithin and entrapment efficiency (EE) of lecithin–chitosan nanoparticles could be increased through the paclitaxel–cholesterol (PTH-CH) complex formulation.[33]

In this article, we have developed the paclitaxel–cholesterol complex-loaded lecithin–chitosan nanoparticles (PTX-CH-loaded LCS_NPs) for intratumoral injection therapy. The PTX-CH-loaded LCS_NPs were prepared and optimized, and the physicochemical properties of nanoparticles were characterized. The 4T1 mouse mammary cancer cell line and its tumor-bearing mice animal model were used to evaluate in vitro and in vivo antitumor efficacy of the nanoparticles via intratumoral injection. The schematic illustrations of PTX-CH-loaded LCS_NPs and their intracellular behavior are shown in Figure 1.

Materials, cell culture, and animals

PTX was bought from Dalian Meilun Biotechnology Co., Ltd. (Dalian, P.R. China). Chitosan (molecular weight 5 W) was obtained from Golden Shell Pharmaceutical Co., Ltd.
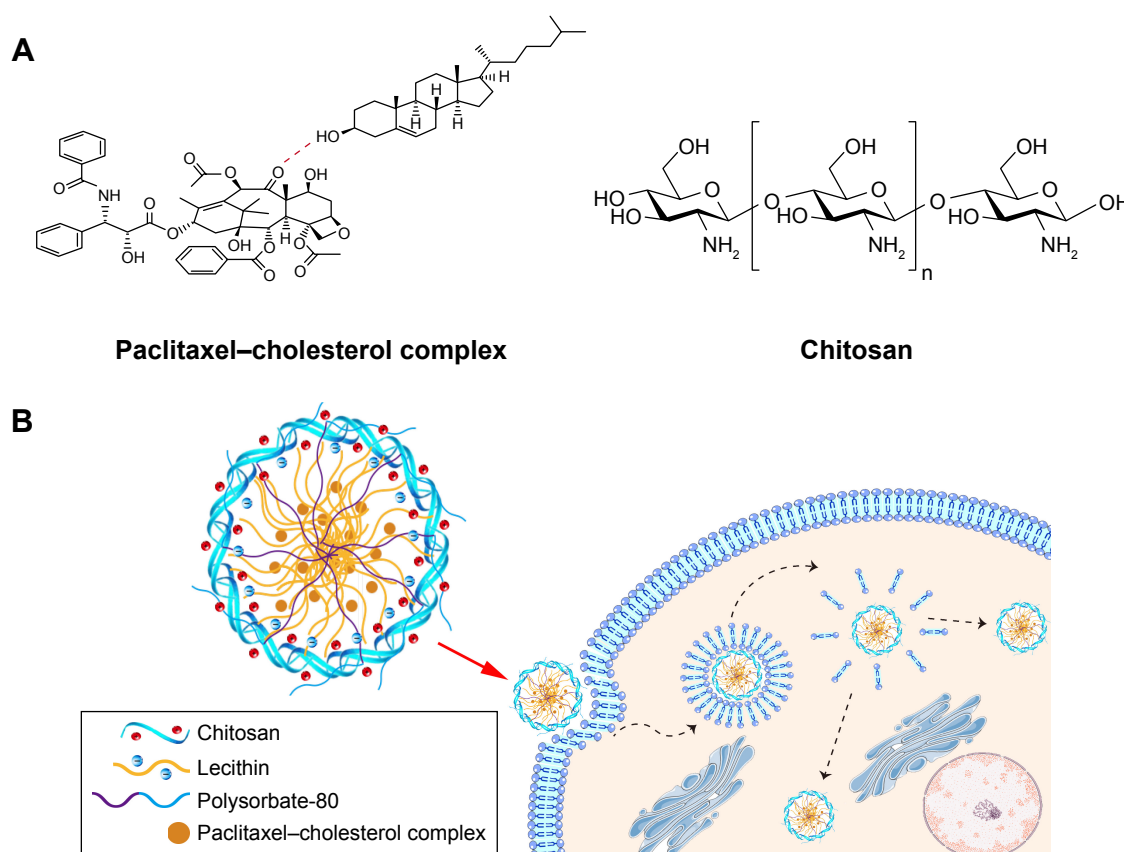
Figure 1 Schematic illustration of PTX-CH-loaded LCS_NPs and their intracellular behavior.
Notes: (**A**) The structural formula of paclitaxel–cholesterol complex and chitosan. (**B**) Schematic illustration of possible structure and intracellular behavior of PTX-CH-loaded LCS_NPs.
Abbreviation: PTX-CH-loaded LCS_NPs, paclitaxel–cholesterol complex-loaded lecithin–chitosan nanoparticles.

(Zhejiang, P.R. China). Soybean lecithin (S75) and cholesterol were bought from Lipoid (Ludwigshafen, Germany). Polysorbate-80 (injection grade) was obtained from Nanjing Well Pharmaceutical Co., Ltd. (Nanjing, P.R. China). Anhydrous ethanol, acetonitrile, and methanol (HPLC grade) were purchased from Sigma-Aldrich Co. (St Louis, MO, USA). Flourescein isothiocyanate/propidium iodide (FITC/PI) apoptosis detection kit and Cell Counting Kit-8 (CCK-8) were bought from Dojindo Laboratories (Kumamoto, Japan). Fetal bovine serum (FBS), RPMI 1640 medium, 0.25% trypsin, and PBS buffer were provided by Thermo Fisher Scientific (Waltham, MA, USA). All the other chemicals were of reagent grade and without further purification.

The 4T1 mouse mammary cancer cell line was provided by the Cell Culture Center of Institute of Basic Medical Sciences, Chinese Academy of Medical Sciences (CAMS). The culture condition was RPMI 1640 medium containing 10% FBS, 5% CO_2, at 37°C. The cells in the logarithmic growth phase were used in all cell experiments. Female BALB/c mice (6 weeks old, 18–22 g) were purchased

from Vital River Laboratory Animal Technology Co., Ltd. (Beijing, P.R. China). All experiments of this project related with animal study were approved by the Institute of Materia Medica in CAMS and Peking Union Medical College (PUMC). The animal experiments also have been approved by the Laboratory Animal Ethics Committee of the Institute of Materia Medica in CAMS and PUMC. We abided the national and institutional principles and protocols for the care and use of experiment animals during the operational procedures of animal experiments.

Preparation of paclitaxel–cholesterol complex

Solvent evaporation method was used to prepare paclitaxel–cholesterol complex (PTX-CH complex) as previously reported by our laboratory.[33] Briefly, PTX and cholesterol (molar ratio 1:1) were dissolved in acetone and refluxed at 40°C for 2 hours. Dried PTX-CH complex was obtained after removal of acetone by evaporation in vacuum. PTX, cholesterol, physical mixture of PTX and cholesterol, and PTX-CH complex were comparatively characterized using

a differential scanning calorimetry (DSC) Analysis (TA Instruments Inc., Sherman, TX, USA).

Preparation of PTX-CH-loaded LCS_NPs

Anhydrous ethanol containing PTX-CH complex and S75 was injected in chitosan solution to prepare PTX-CH-loaded LCS_NPs using the solvent-injection method reported.[34] Chitosan solution was prepared through 1 g chitosan dissolved in 100 mL 1% acetic acid water solution. Then, 4 mL anhydrous ethanol with different concentration of PTX-CH complex was injected into 46 mL distilled water that contained chitosan and polysorbate-80 at different ratios during continuous magnetic stirring to obtain PTX-CH-loaded LCS_NPs.

Physicochemical characterization of PTX-CH-loaded LCS_NPs

The particle size, polydispersity index (PDI), and zeta potential of PTX-CH-loaded LCS_NPs were measured by dynamic light scattering and electrophoretic light scattering (Zetasizer Nano ZS90; Malvern Instruments Ltd., Malvern, UK). The morphology of PTX-CH-loaded LCS_NPs was observed under a transmission electron microscope (Hitachi H-7650; Hitachi Ltd., Tokyo, Japan).

Entrapment efficiency of PTX-CH-loaded LCS_NPs

EE% of PTX-CH-loaded LCS_NPs was determined using the minicolumn centrifugation technique in order to separate the prepared nanoparticles from the free drug.[35] Briefly, 0.5 mL LCS_NPs solution was dripped into a minicolumn filled with Sephadex G-50 and centrifuged (500 rpm, 0.5 minute) to distribute the suspension in the minicolumn. After that, the minicolumn was washed with 0.5 mL distilled water three times (1,000 rpm, 1 minute). The free drug that remained in the Sephadex G-50 minicolumn and drug-loaded nanoparticles were flowed out with elutes that were collected and adjusted to 10 mL by anhydrous ethanol. The sample was filtered by 0.22 μm microporous membrane after the nanoparticles were broken down thoroughly by ultrasound for 10 minutes. Finally, entrapped PTX was determined at 227 nm using an HPLC system (Agilent 1260 infinity; Agilent Technologies, Santa Clara, CA, USA). The column was a GRACE Allsphere ODS-2 C18 (5 μm, 250×4.6 mm), and the mobile phase was acetonitrile–methanol–water (36:23:41), the injection volume of the sample was 10 μL, the flow rate was 1 mL/min and column temperature was set

at 25°C. EE% and drug loading (DL%) PTX in the LCS_NPs were calculated as follows:[36]

$$EE\% = \frac{\text{Weight of encapsulated drug}}{\text{Weight of initial drug}} \times 100\%$$

$$DL\% = \frac{\text{Weight of initial drug}}{\text{Total volume on NPs solution}} \times 100\%$$

In vitro paclitaxel release assay

The in vitro release of PTX of PTX-CH-loaded LCS_NPs was evaluated with the dialysis diffusion technique.[37] To increase the concentration of nanoparticles to obtain the release assay samples, a centrifugal filter tube (100 K MWCO; Millipore, Billerica, MA, USA) was used. The LCS_NPs suspension was placed in the filter tube and centrifuged (4,000 rpm, 12 minutes). Finally, the content of PTX in LCS_NPs suspension was adjusted to 0.5 mg/mL through HPLC analysis. Two samples of concentrated LCS_NPs solution (0.5 mL, 0.5 mg/mL) and one sample of PTX solution (0.5 mL, 0.5 mg/mL) were added into a dialysis bag (12 kDa). The bags were immersed in 30 mL sodium salicylate solution (1 M, pH 7.4) or 30 mL sodium salicylate solution (1 M, pH 5.8), and were shacked at 100 rpm, 37°C. A measured quantity of 0.5 mL sodium salicylate solution was taken out and replaced with 0.5 mL fresh solution at each time interval. The content of PTX in each sample was detected by the above established HPLC method after being centrifuged (12,000 rpm, 10 minutes). Finally, the accumulative release of PTX was calculated and plotted.

Cellular uptake analysis

PTX in LCS_NPs was replaced by coumarin-6 (C6) to observe and analyze cellular uptake and localization of LCS_NPs. 15×10^4/well tumor cells were put in six-well plates with coverslips at the bottom and incubated for 24 hours. Then, the cells were cultured with fresh medium containing C6-loaded LCS_NPs or free C6 (1 μg/mL) for 5, 15, 30, and 60 minutes. After being washed with cold PBS buffer three times to remove excess C6-loaded LCS_NPs or free C6, the cells were fixed with 4% paraformaldehyde solution, washed and stained with DAPI for another 10 minutes. The cells were finally observed through a confocal fluorescence microscope (Carl Zeiss LSM 710; Carl Zeiss Microscopy, Jena, Germany). The seeded cells were cultured with fresh medium containing C6-loaded LCS_NPs or free C6 for 15, 60, and 120 minutes, and analyzed with a FACSCalibur flow cytometer (Becton Dickinson, Franklin Lakes, NJ, USA)

to quantify the amount of C6-loaded LCS_NPs taken up by cells.

To explore the uptake pathways of C6-loaded LCS_NPs, several membrane entry inhibitors were examined. The cells were seeded in a 12-well plate with 15×10^4/well. After attachment, the cells were cultured with chlorpromazine (10 µg/mL), colchicine (4 µg/mL), brefeldin A from penicillium brefeldianum (BFA, 5 µg/mL), Filipin (5 µg/mL), NaN_3 (3 mg/mL), methyl-β-cyclodextrin (M-β-CD, 5 mg/mL), respectively. Then, the cells were treated with C6-loaded LCS_NPs (1 µg/mL). The cells were collected and analyzed with flow cytometer analysis.

Cell viability assay

CCK-8 assays were performed to evaluate the cytotoxicity of polymer and the cytotoxicity of PTX-CH-loaded LCS_NPs on 4T1 cells. In brief, 4T1 tumor cells were cultured 24 hours for attachment in 96-well plates at a density of 5×10^3 cells/well, and then were treated and cultured in various concentrations of blank LCS_NPs for 48 hours to evaluate the cytotoxicity of polymer. The blank group was treated with culture medium alone. According to CCK-8 kit instructions, the cells were cultured in CCK-8 reagent for another 2 hours, and were measured at 490, 650 nm by a Synergy H1 Microplate Reader (BioTek, Dallas, TX, USA). Cytotoxicity of PTX-CH-loaded LCS_NPs was detected by CCK-8 assay, too. Cells of the same concentration were cultured with different concentrations of PTX-CH-loaded LCS_NPs based on PTX, and were cultured for 24 or 48 hours. After being treated with CCK-8 reagent, the OD values were measured. The cells untreated with PTX served as controls and cell viability was calculated.

Cell apoptosis assay

The apoptosis of 4T1 cells caused by PTX-CH-loaded LCS_NPs was quantitatively analyzed by Annexin V-FITC/PI double staining assay. The 4T1 cells were seeded in 6-well plates (15×10^4/well) and cultured for 24 hours. The cells were washed twice in each well after treatment with culture medium containing PTX-CH-loaded LCS_NPs or PTX solution for 24 hours, gathered and centrifuged, dispersed in binding buffer, and treated according to the Annexin V-FITC and PI staining manufacturer's protocol. The samples were analyzed by the FACSCalibur flow cytometer.

Antitumor evaluation of PTX-CH-loaded LCS_NPs by intratumoral injection in vivo

The 4T1 cell line is a mouse mammary cancer cell line; so, we established the tumor-bearing model with female BALB/c mice (6 weeks old, 18–22 g) via subcutaneous injection of tumor cells, with 15×10^4 cells into the fourth mammary pad. We measured the weight and tumor size of the mice every other day until the volume of tumors reached about 150 mm^3. The tumor-bearing mice were grouped randomly (n=6), as follows: saline, blank LCS_NPs, PTX, and PTX-CH-loaded LCS_NPs. The four groups were administered four times by intratumoral injection every 3 days. In PTX and PTX-CH-loaded LCS_NPs group, PTX was administered at the dose of 5 mg/kg, much lower than that of intravenous administration, 10 or 15 mg/kg.[38] All these groups were treated four times by intratumoral injection every 3 days, and we measured tumor volumes and body weights every other day. Tumor volumes were calculated according to the following formula: $W^2\times L/2$ (W represents the minor diameter and L represents the major diameter). All tumor-bearing mice were killed 3 days after the last administration by cervical dislocation. The tissues (liver, lung) were treated with 4% formaldehyde tissue fixative and stained with H&E. The tumors of tumor-bearing mice in each group were isolated, weighed, photographed in group, and finally stored in 4% formaldehyde tissue fixative to be stained with H&E. TUNEL assay was used to distinguish the apoptosis cells in the tumor tissue. The tumor tissues were treated with a TUNEL-POD kit according to the instructions. The H&E and TUNEL slides of the tissues and tumors were photographed by an optical microscope (Leica DM4000B; Leica Microsystems, Wetzlar, Germany).

Survival analysis

The 4T1 tumor-bearing mice model was established with the same method mentioned above. Forty tumor-bearing mice were grouped randomly (n=10) including saline group, blank LCS_NPs group, PTX group, and PTX-CH-loaded LCS_NPs group. The mice in these four groups were administered four times via intratumoral injection every 3 days until they died. Survival curves were plotted using GraphPad Prism software (version 5.0.0.0; GraphPad Software Inc., La Jolla, CA, USA).

Statistical analysis

Statistical analysis in this paper was conducted using SPSS 22 (IBM Corporation, Armonk, NY, USA). The results in this article are shown as mean ± SD. Statistical comparisons were analyzed to determine group differences through ANOVA by SPSS 22. Student's t-test was used to evaluate significant difference between two groups, indicated as follows: *$P<0.05$, **$P<0.01$, ***$P<0.001$.

Results and discussion

Preparation of paclitaxel–cholesterol complex

In this study, PTX-CH complex was prepared to improve the solubility of PTX in the phospholipid, to improve drug EE of PTX-CH-loaded LCS_NPs, and to increase the stability of the LCS_NPs.[33,39] DSC was used to analyze interactions between PTX and cholesterol in the complex. In Figure 2, DSC curves of the samples, the endothermal peaks of PTX (A) and cholesterol (B) were 222.58°C and 146.83°C,
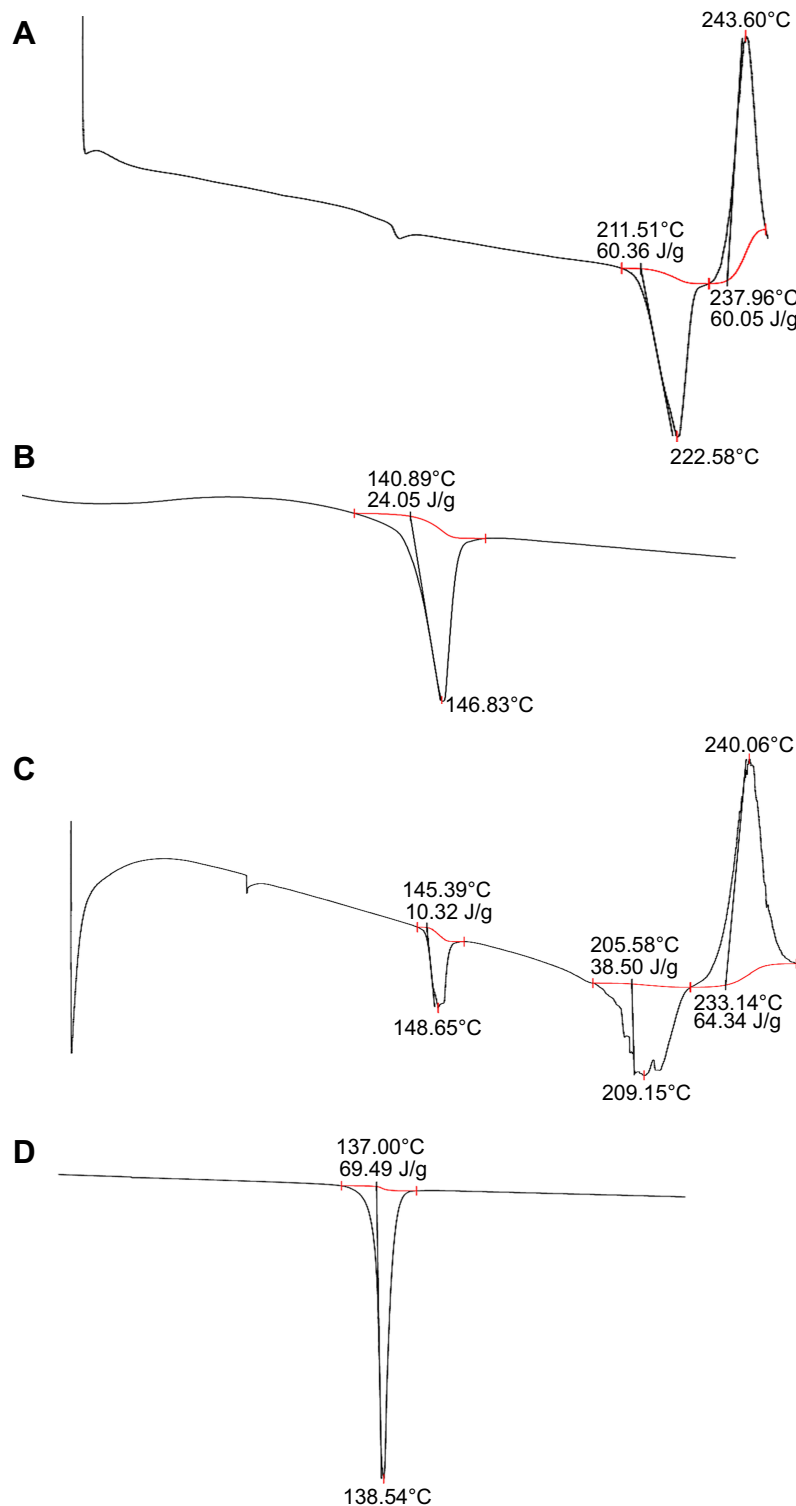

Figure 2 The results of DSC test of PTX (**A**), cholesterol (**B**), physical mixture of PTX and cholesterol (**C**), and PTX-CH complex (**D**).
Abbreviations: DSC, differential scanning calorimetry; PTX, paclitaxel; PTX-CH complex, paclitaxel–cholesterol complex.

Table 1 Effect of lecithin:chitosan (w:w) on nanoparticles

L/CS ratio (w/w)	Size[a] (nm)	PDI[a]	Zeta potential[a] (+mV)	EE[a] (%)	DL[a] (µg/mL)	Stability (24 hours)
5:1	230.00±2.60	0.37±0.05	25.57±1.57	93.60±0.54	143.39±0.72	–
10:1	162.33±1.27	0.27±0.00	23.10±0.20	91.75±0.23	128.31±0.4	–
20:1	142.77±0.91	0.25±0.01	13.30±0.17	92.17±1.35	125.22±2.55	–
40:1	124.43±1.27	0.28±0.00	9.92±0.51	92.08±0.58	132.44±0.40	–
80:1	120.60±1.23	0.28±0.00	4.70±0.13	92.33±0.80	125.36±1.16	–

Note: (–) means stable in 24 hours; [a]mean ± SD (n=3).
Abbreviations: DL, drug loading; EE, entrapment efficiency; L/CS, lecithin/chitosan; PDI, polydispersity index.

respectively. There were two endothermal peaks of PTX at 209.15°C and cholesterol at 148.65°C of the physical mixture of PTX and cholesterol (C). The endothermal peak of PTX was <222.58°C. As the temperature rose during DSC test, PTX and cholesterol formed the complex partially. The endothermal peak of PTX-CH complex (D) was 138.54°C and a broad one. The peaks of PTX and cholesterol disappeared. This indicated that the PTX-CH complex was successfully prepared.[33,40]

Preparation and characterization of PTX-CH-loaded LCS_NPs

According to the solvent-injection method established previously,[24] the nanoparticles of PTX-CH-loaded LCS_NPs were prepared and optimized. Briefly, an anhydrous ethanol containing S75 and PTX-CH complex was injected into the stirring chitosan solution. The nanoparticles composed of lecithin and chitosan had a round appearance and satisfactory stability when ratio of lecithin to chitosan was about 20:1 (w/w) in previous studies.[24,41,42] Polysorbate-80 was chosen to increase drug solubility, and stabilize the nanosystem.[43] To evaluate the best formulation for PTX-CH-loaded LCS_NPs, we used different L/CS ratios (w/w) (5:1, 10:1, 20:1, 40:1, and 80:1) to determine the optimal L/CS ratio with 10 mg PTX-CH complex loading. Considering the changes of particle sizes, PDIs, and zeta potentials caused by L/CS ratios (w/w), as is shown in Table 1, we chose the L/CS ratio 20:1 in subsequent experiments. Next, we investigated the effect of polysorbate-80 on EEs and DLs of LCS_NPs in

different concentrations (1%, 2%, 3%, and 4%), as shown in Table 2. As the content of polysorbate-80 ranged from 1% to 4% (w/v), the EEs were increased from 79.68% to 94.60%, but the particle size and PDI of LCS_NPs were the smallest when the concentration of polysorbate-80 was 2%. The result indicated that polysorbate-80 served as a surfactant in the LCS_NPs at lower concentrations such as 1% and 2%, but polysorbate-80 would destroy the structure of LCS_NPs and form micelles with PTX as its concentration increased. This might account for the increased value of PDI and EE as the concentration changed. Finally, we explored the influence of drug dosage on LCS_NPs preparation, as shown in Table 3. The LCS_NPs were unstable within 24 hours when the content of PTX-CH complex exceeded 15 mg. Therefore, the optimal formulation for PTX-CH-loaded LCS_NPs was the L/CS ratio of 20:1 (w/w), 2% polysorbate-80 in aqueous solution, and 15 mg PTX-CH complex in anhydrous ethanol.

The morphology of PTX-CH-loaded LCS_NPs was observed under transmission electron microscopy. The LCS_NPs exhibited a sphere-like shape (Figure 3A). The average particle size and PDI under optimal conditions were 142.83±0.25 nm and 0.26±0.01, respectively (Figure 3B). PTX-CH-loaded LCS_NPs had a positive zeta potential of 13.50±0.20 mV (Figure 3C), which suggested that the LCS_NPs were positively charged. The zeta potential of LCS_NPs was about 14 mV, but the LCS_NPs remained relatively stable during the 3 days of storage at 4°C without notable change in particle size of PTX-CH-loaded LCS_NPs (Figure 3D and E; Table 4).

Table 2 The effect of the amount of Polysorbate-80 on nanoparticles

Polysorbate-80 (w/v)	Size[a] (nm)	PDI[a]	Zeta potential[a] (+mV)	EE[a] (%)	DL[a] (µg/mL)	Stability (24 hours)
1%	194.67±2.55	0.44±0.02	17.23±0.32	79.68±0.18	133.55±0.66	–
2%	137.63±0.55	0.26±0.00	11.03±0.40	91.58±0.59	117.80±0.23	–
3%	152.13±4.14	0.30±0.01	11.60±0.17	92.12±0.72	126.08±0.84	–
4%	142.63±6.24	0.52±0.04	12.00±0.20	94.60±0.84	132.14±0.52	–

Note: [a]Mean ± SD (n=3), (–) means stable in 24 h.
Abbreviations: DL, drug loading; EE, entrapment efficiency; PDI, polydispersity index.

Table 3 Effect of the amount of PTX-CH complex on nanoparticles

PTX-CH complex (mg)	Size[a] (nm)	PDI[a]	Zeta potential[a] (+mV)	EE[a] (%)	DL[a] (µg/mL)	Stability (24 hours)
10	143.13±1.97	0.26±0.01	14.47±0.47	92.46±0.27	122.23±0.51	−
15	141.20±0.90	0.27±0.01	14.10±1.30	91.86±0.26	195.06±0.66	−
20	140.37±0.65	0.25±0.01	12.73±0.80	92.12±0.92	262.79±0.42	+

Note: (−) means stable in 24 hours, (+) means instable in 24 hours; [a]mean ± SD (n=3).
Abbreviations: DL, drug loading; EE, entrapment efficiency; PDI, polydispersity index; PTX-CH complex, paclitaxel–cholesterol complex.

In vitro paclitaxel release assay

The drug release study was evaluated in the different release media at pH 5.8 and 7.4, and the results suggested that the release of PTX from PTX-CH-loaded LCS_NPs showed a pH-sensitive pattern compared with PTX (Figure 4). The release of PTX from PTX group reached 47.6% at 12 hours, and the drug release from LCS_NPs at pH 5.8 and 7.4 was 41.2% and 34.1%, respectively. This suggested that the LCS_NPs had a sustained release effect. After 84 hours, the accumulative drug release from LCS_NPs at pH 5.8 was 64.4%, but at pH 7.4 the release rate was only 47.7%. The above results indicated that the drug release from LCS_NPs was quicker and more thorough in an acidic environment. The purpose of PTX-CH complex preparation was to increase the solubility of PTX in lecithin as mentioned above. LCS_NPs as a carrier of PTX-CH complex embedded in lecithin were electrostatic and self-assembled by positively charged chitosan and negatively charged lecithin. When LCS_NPs
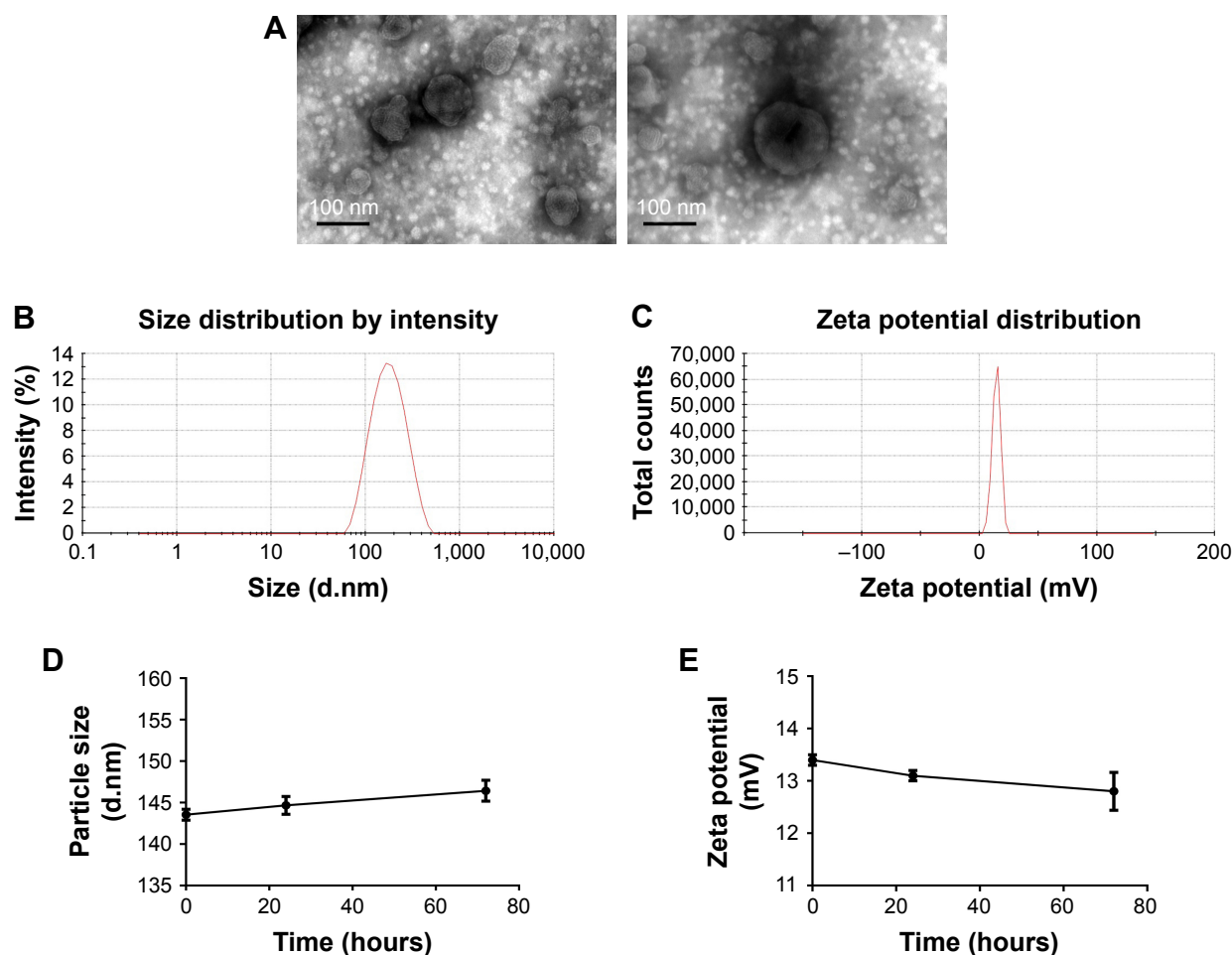

Figure 3 Characterizations of PTX-CH-loaded LCS_NPs.
Notes: (**A**) TEM image of PTX-CH-loaded LCS_NPs (scale bar was 100 nm). (**B**) Size distribution of PTX-CH-loaded LCS_NPs. (**C**) Zeta potential of PTX-CH-loaded LCS_NPs. (**D**) Particle size change of PTX-CH-loaded LCS_NPs within 3 days. (**E**) Zeta potential change of PTX-CH-loaded LCS_NPs within 3 days.
Abbreviations: PTX-CH-loaded LCS_NPs, paclitaxel–cholesterol complex-loaded lecithin–chitosan nanoparticles; TEM, transmission electron microscopy.

Table 4 Stability of PTX-CH-loaded LCS_NPs within 3 days

Storage time (days)	Particle size[a] (nm)	Zeta potential[a] (+mV)
1	143.54±0.65	13.42±0.11
2	144.67±1.07	13.10±0.14
3	146.43±1.27	12.80±0.36

Note: [a]Mean ± SD (n=3).
Abbreviation: PTX-CH-loaded LCS_NPs, paclitaxel–cholesterol complex-loaded lecithin–chitosan nanoparticles.

were in an acidic environment, the –NH$_2$ and –OH of chitosan might interact with H$^+$ in acidic solution, which might lead to the changes in molecule conformation of chitosan and charge stability on the surface of LCS_NPs. All these might account for the destruction of LCS_NPs and accelerated drug release in an acidic environment. Studies have shown that the tumor extracellular pH is around 5.8–7.2,[44,45] as the pH value of the normal tissue microenvironment is around 7.4. Therefore, PTX-CH-loaded LCS_NPs exhibited a pH-sensitive tumor-targeting property because of the lower pH microenvironment in tumor tissues, and consequently could reduce chemotherapy-induced damage to normal tissues and organs. PTX could enter into tumor cells by diffusion after release from LCS_NPs outside cells or by endocytosis in LCS_NPs. The PTX release of PTX-CH-loaded LCS_NPs taken into cells by endocytosis could also be triggered in the low pH endosomes (pH 5.0–6.5) and lysosomes (pH 4.0–5.0).[20]

Cellular uptake studies

In the course of observation of the cellular uptake of LCS_NPs in tumor cells, PTX-CH complex in PTX-CH-loaded
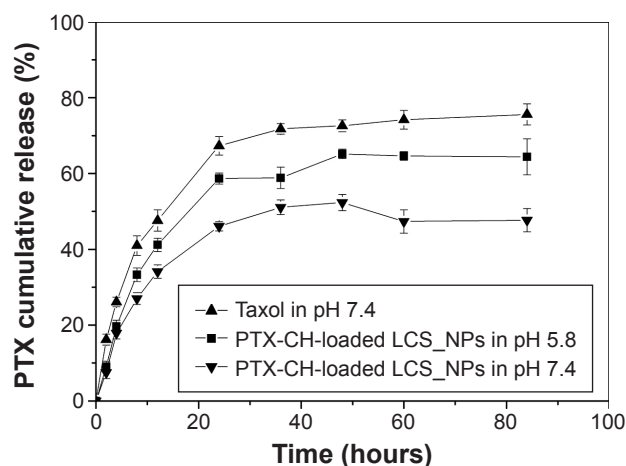

Figure 4 The study of release behavior of PTX-CH-loaded LCS_NPs in vitro.
Note: The release of paclitaxel from PTX-CH-loaded LCS_NPs at pH 5.8 and pH 7.4 compared with PTX solution.
Abbreviations: PTX, paclitaxel; PTX-CH-loaded LCS_NPs, paclitaxel–cholesterol complex-loaded lecithin–chitosan nanoparticles.

LCS_NPs was replaced by the fluorescent probe C6 to prepare C6-loaded LCS_NPs. The blue and green fluorescence signals represented the cell nuclei stained with DAPI and C6, respectively (Figure 5A). The signals of C6 could be observed after incubation with C6-loaded LCS_NPs for 5 minutes and the signals at 15, 30, and 60 minutes became stronger, while the signals of free C6 group could not be observed clearly until incubation for 60 minutes. This suggested that the cellular uptake of LCS_NPs was more efficient than that of the free drug. The result also confirmed that PTX could be delivered by PTX-CH-loaded LCS_NPs into cells. The intracellular efficiency of C6-loaded LCS_NPs was measured quantitatively by flow cytometry. As shown in Figure 5B and C, which was similar to the observation with confocal laser scanning microscopy, the intracellular efficiency of C6-loaded LCS_NPs was much stronger than that of free C6. The mean fluorescence intensity of the NPs reached a high level at 15 minutes, and it was basically saturated at 60 minutes. The result further indicated that the PTX delivery of PTX-CH-loaded LCS_NPs was more efficient compared with single-drug delivery. The nanoparticles showed more efficient drug delivery into cancer cells, which might be due to the EPR effect.[22]

On the other hand, the possible endocytic pathways of LCS_NPs were investigated via different inhibitors. We investigated the identified endocytic pathways for macromolecules (Figure 6),[46] including clathrin-mediated endocytosis, macropinocytosis, and caveolae-mediated endocytosis, and analyzed them by flow cytometry. Chlorpromazine is one of the inhibitors of clathrin-mediated endocytosis, which dissociates clathrin from the surface membrane to inhibit coated pit endocytosis.[47] The cellular uptake of C6-loaded LCS_NPs after treatment with chlorpromazine stayed at almost the same level as the control (P>0.05), indicating that there was little participation of clathrin-mediated endocytosis in endocytosis. Macropinocytosis, which is typically inhibited by colchicine,[48] refers to the formation of large and irregular primary endocytic vesicles. The cellular uptake of LCS_NPs was reduced by colchicine by about 43%, suggesting that macropinocytosis might participate in cellular uptake of LCS_NPs. Filipin is a selective inhibitor of caveolae formation to inhibit caveolae-mediated endocytosis.[49] The cellular uptake of LCS_NPs into cells treated with Filipin was reduced by 82%. This indicated that caveolae-mediated endocytosis and macropinocytosis were both involved in LCS_NPs uptake, as was shown by previous research about the cellular uptake mechanism of chitosan nanoparticles.[50,51] The energy dependence of the macropinocytosis pathway was
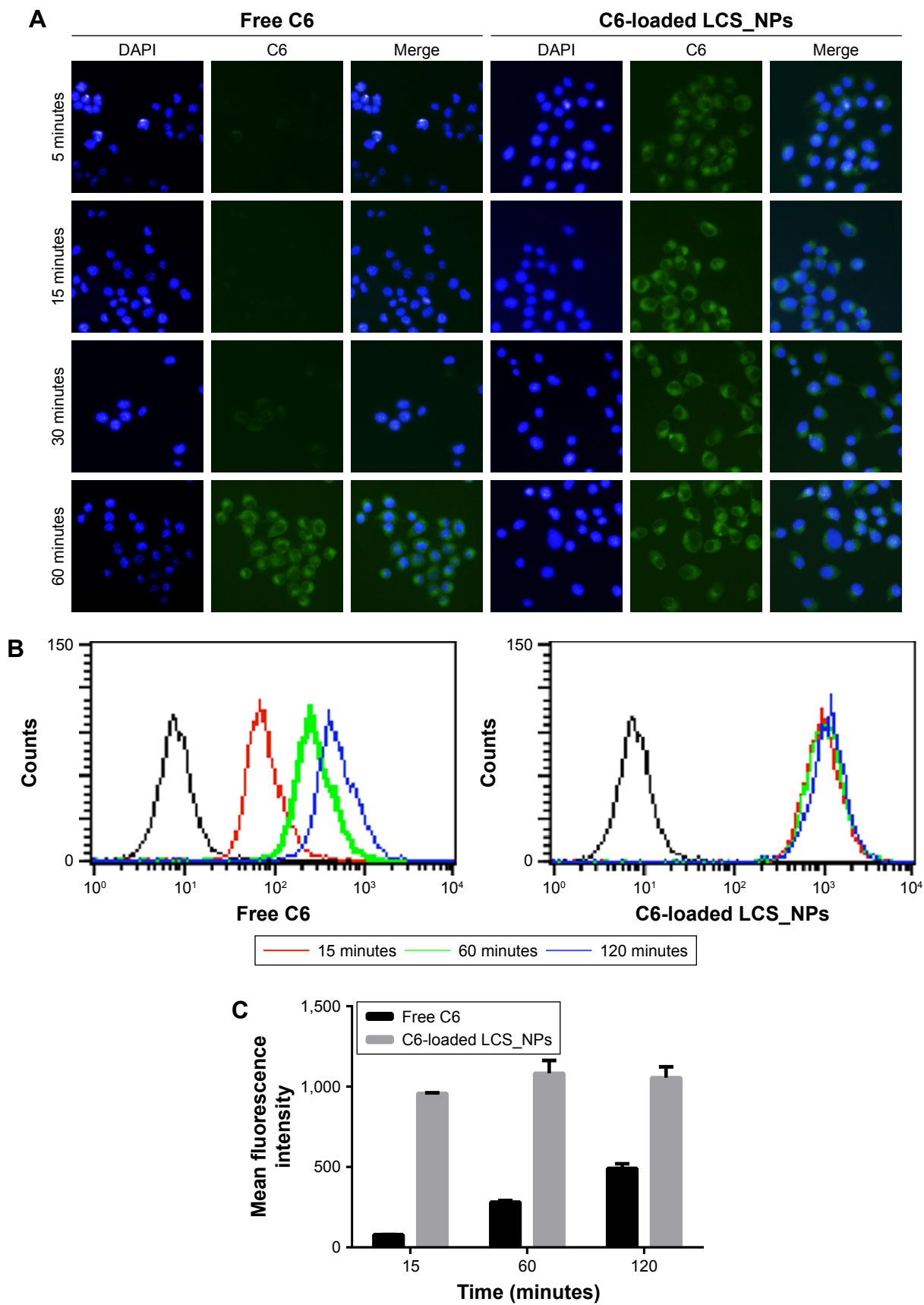
Figure 5 Cellular uptake studies of LCS_NPs.

Notes: (**A**) Observation of 4T1 cells by confocal microscopy after treatment with free C6 or C6-loaded LCS_NPs for 5, 15, 30, and 60 minutes, respectively. (**B**, **C**) Quantitative analysis of free C6 or C6-loaded LCS_NPs uptake by flow cytometry after incubation with free C6 or C6-loaded LCS_NPs for 15, 60, and 120 minutes.

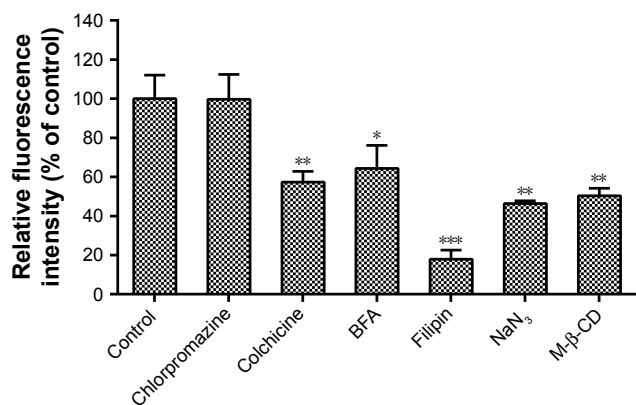**Abbreviations:** C6, coumarin-6; C6-loaded LCS_NPs, coumarin-6-loaded lecithin–chitosan nanoparticles.

Figure 6 Cellular uptake analysis of C6-loaded LCS_NPs after incubation with different endocytic inhibitors by flow cytometry.
Notes: 4T1 cells were cultured in serum-free medium for 1 hour containing chlorpromazine (10 μg/mL), colchicine (4 μg/mL), BFA (5 μg/mL), Filipin (5 μg/mL), NaN$_3$ (3 mg/mL), M-β-CD (5 mg/mL), respectively. Before flow cytometry analysis, cells were cultured with C6-loaded LCS_NPs (1 μg/mL) for another 1 hour (n=3, mean ± SD). *$P<0.05$ vs control, **$P<0.01$ vs control, ***$P<0.001$ vs control.
Abbreviations: BFA, brefeldin A from penicilliumbrefeldianum; C6-loaded LCS_NPs, coumarin-6-loaded lecithin–chitosan nanoparticles; M-β-CD, methyl-β-cyclodextrin.

confirmed by culturing the cells with sodium azide (NaN$_3$) before the addition of LCS_NPs.[52] The inhibitor, NaN$_3$, also decreased LCS_NPs uptake by >50%. Lipid rafts assisted in membrane trafficking and are located in cell membranes.[51] To investigate the influence of lipid rafts on cellular uptake of LCS_NPs, cells treated with M-β-CD as the inhibitor of lipid rafts[53] significantly diminished the fluorescence intensity (about 50%) compared with the control, indicating the participation of cholesterol and lipid rafts in the uptake of LCS_NPs. The cells were treated with penicillium brefeldianum (BFA) to investigate whether Golgi apparatus participated in the transportation of LCS_NPs.[54] The fluorescence intensity of cells treated with BFA was diminished by about 36%, showing that Golgi apparatus participated in the transportation of LCS_NPs in cells. The results suggested that C6-loaded LCS_NPs entered cells via energy-dependent endocytosis, including caveolae-mediated endocytosis and macropinocytosis, with the participation of the Golgi apparatus.

Cell viability assay

The cytotoxicity of blank LCS_NPs against 4T1 cells was evaluated by CCK-8 assay, and the concentrations of LCS_NPs were equivalent of PTX-CH-loaded LCS_NPs ranging from 0.01 to 5 μg/mL (Figure 7A). Little cytotoxicity was observed as the concentrations of blank LCS_NPs increased. The results suggested that blank LCS_NPs showed almost no cytotoxicity as a drug delivery carrier with good safety and biocompatibility.

CCK-8 assay was also used to evaluate the inhibitory capacity of PTX-CH-loaded LCS_NPs against cell proliferation

after incubation for 24 and 48 hours compared with PTX solution. Results in Figure 7B showed that PTX-CH-loaded LCS_NPs could inhibit cell proliferation more effectively at lower concentrations of PTX ranging from 0.01 to 0.05 μg/mL and after 24 and 48 hours of incubation compared with PTX solution. But, as the concentration increased, the difference of inhibitory capacity between PTX-CH-loaded LCS_NPs and PTX solution was not significant, because of the increased cytotoxicity of PTX solution. The results suggested that PTX-CH-loaded LCS_NPs had a better inhibitory capacity at a lower concentration than PTX solution, which was conducive to intratumoral injection therapy.

Influence of PTX-CH-loaded LCS_NPs on cell apoptosis

4T1 cells were cultured with blank LCS_NPs, PTX-CH-loaded LCS_NPs, or PTX solution for 24 hours, and then the cells treated with Annexin V-FITC/PI were analyzed to distinguish the apoptotic cells by flow cytometry (Figure 8). The 4T1 cells cultured with blank LCS_NPs showed 6.03% apoptosis, while the control group had 6.05% apoptotic cells, indicating that the blank LCS_NPs had little influence on cell progression. Meanwhile, the apoptotic rate in PTX-CH-loaded LCS_NPs group was 72.68%, which was significantly increased compared with PTX solution group (39.21%). The antitumor mechanism of PTX is the inducement of G2/M arrest in cell cycle.[55] The data of the cell apoptosis analysis suggested that PTX-CH-loaded LCS_NPs could induce apoptosis of tumor cells more effectively.

In vivo antitumor efficacy of PTX-CH-loaded LCS_NPs

4T1 tumor-bearing BALB/c mice were selected as an animal tumor model to evaluate antitumor efficacy of PTX-CH-loaded LCS_NPs in vivo. The tumor-bearing mice with an average tumor volume of 150 mm^3 were grouped randomly (saline, blank LCS_NPs, PTX, PTX-CH-loaded LCS_NPs, n=6). The mice were treated four times by intratumoral injection every 3 days. The tumors were monitored and measured every other day. As shown in Figure 9A, the tumor volumes of tumor-bearing mice treated with saline and blank LCS_NPs were growing rapidly. In contrast, the tumors were significantly inhibited when treated with PTX and PTX-CH-loaded LCS_NPs, especially the latter. The tumors of the four groups were dissected and weighed at 3 days after the last administration (Figure 9B and C). The average weight of tumor in PTX-CH-loaded LCS_NPs group was smaller than that in PTX group with a significant difference ($P<0.05$), not to mention saline and blank LCS_NPs group.
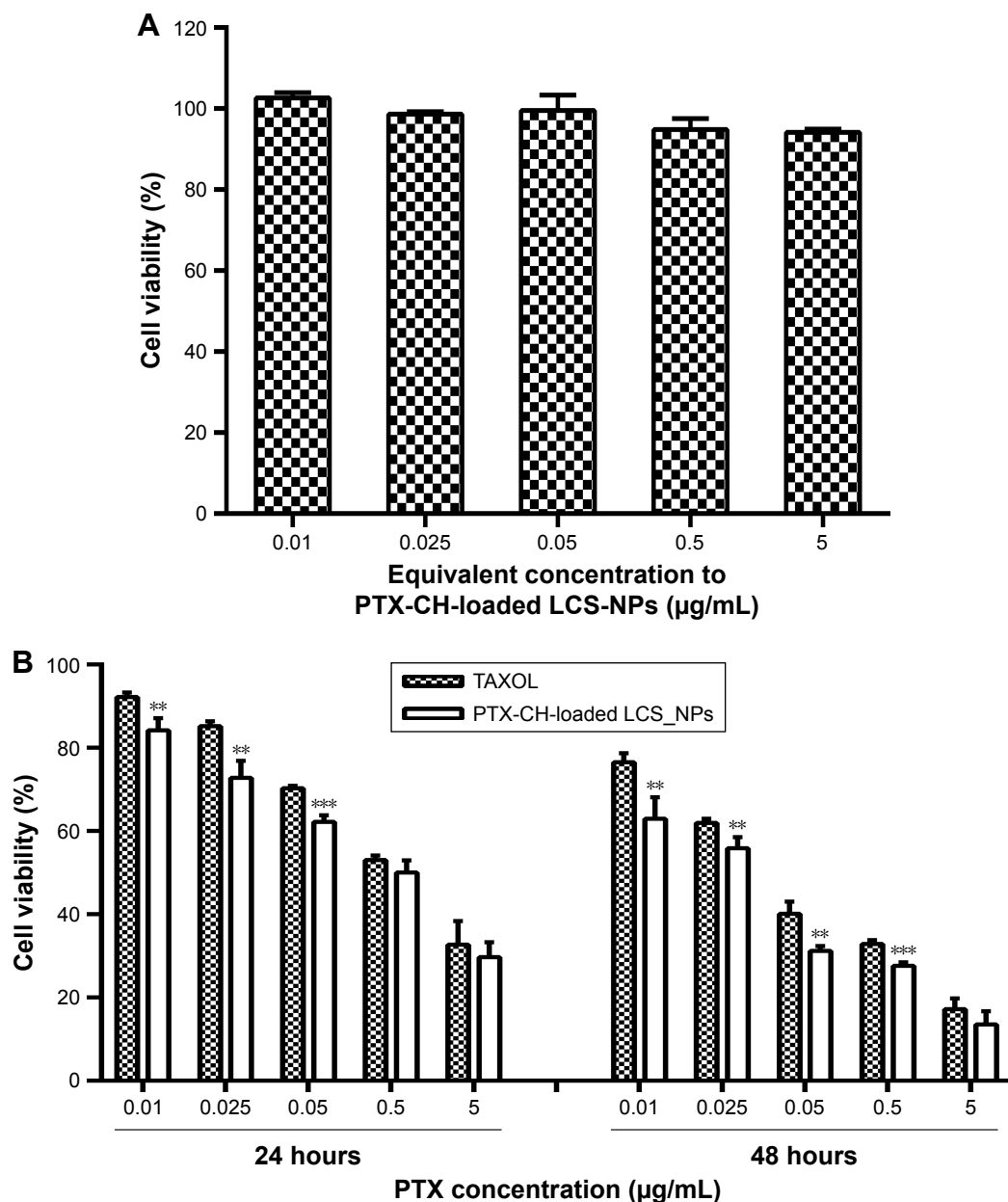
Figure 7 (**A**) Cytotoxicity of blank LCS_NPs for 4T1 cells (n=4, mean ± SD). (**B**) Inhibitory capacity of PTX-CH-loaded LCS_NPs against cell proliferation after incubation of 24 or 48 hours compared with PTX (n=4, mean ± SD). **$P<0.01$ vs PTX, ***$P<0.001$ vs PTX.
Abbreviations: PTX, paclitaxel; PTX-CH-loaded LCS_NPs, paclitaxel–cholesterol complex-loaded lecithin–chitosan nanoparticles.

These results suggested that PTX-CH-loaded LCS_NPs showed better inhibitory efficacy by intratumoral injection than PTX. The results of TUNEL assay (Figure 10) showed that the number of tumor cells in both PTX group and PTX-CH-loaded LCS_NPs group decreased. There were more apoptotic tumor cells (the brown ones, red arrow pointed) in PTX-CH-loaded LCS_NPs group than in the other three groups. The result indicated that PTX-CH-loaded LCS_NPs could deliver PTX more effectively and rapidly into tumor cells to inhibit the growth of tumor by inducing cell apoptosis.

The results of TUNEL assay were consistent with antitumor study in vivo. The above release test results confirmed that PTX delivery of PTX-CH-loaded LCS_NPs into tumor cells was more efficient, due to their pH-sensitive release manner and highly efficient endocytosis of LCS_NPs included caveolae-mediated endocytosis and macropinocytosis with the participation of the Golgi apparatus, endosomes, or lysosomes. In the endolysosomal pH range, the buffering capacity of chitosan was higher than that of polyethyleneimine (PEI). And the endosomal escape capacity of chitosan was similar to
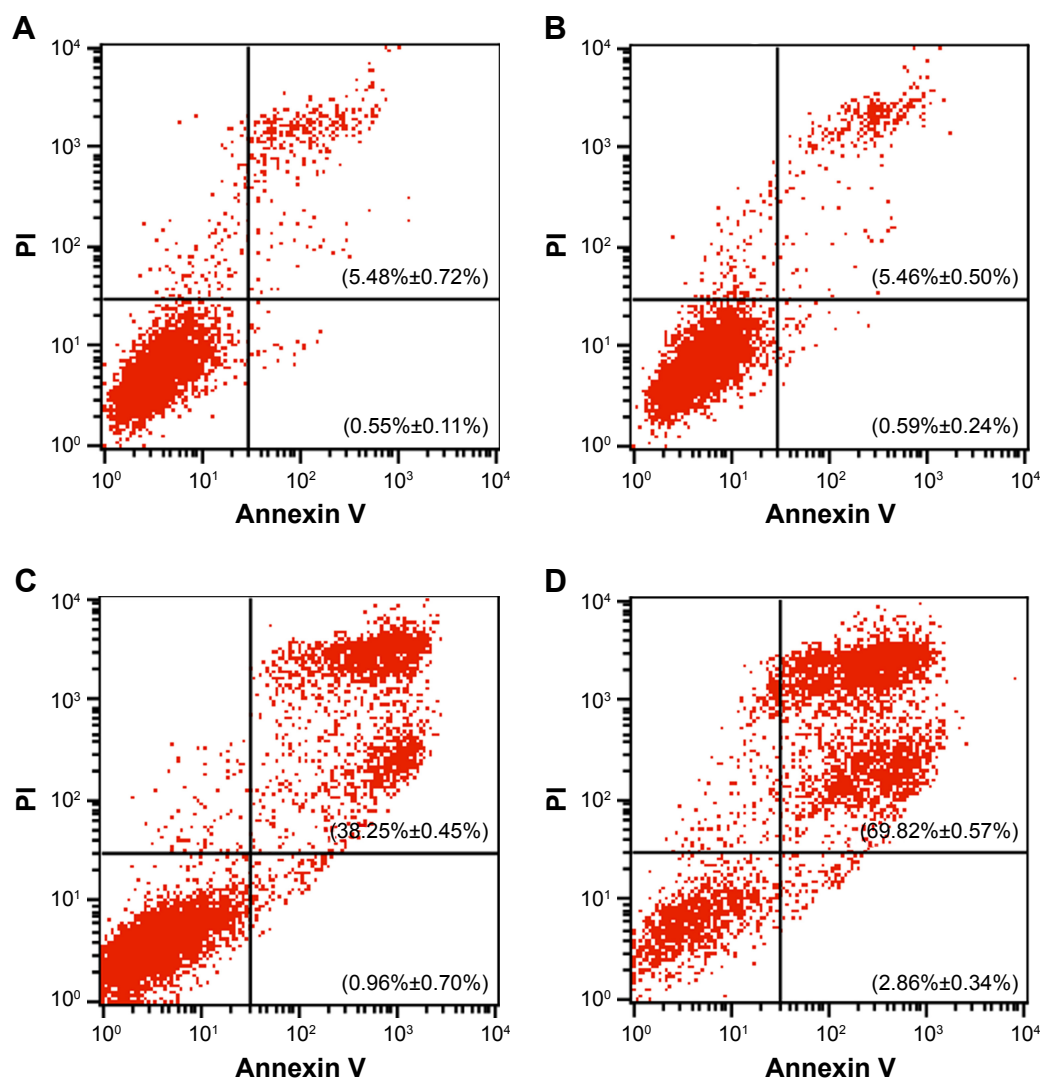
Figure 8 Influence of PTX-CH-loaded LCS_NPs on cell apoptosis analyzed by flow cytometry.
Notes: (**A**) Control group of 4T1 cells without any treatment. (**B**) Blank group of 4T1 cells cultured with blank LCS_NPs. (**C**) PTX group of 4T1 cells cultured with PTX solution. (**D**) NPs group of 4T1 cells cultured with PTX-CH-loaded LCS NPs (n=3, mean ± SD).
Abbreviations: LCS_NPs, lecithin–chitosan nanoparticles; PI, propidium iodide; PTX-CH-loaded LCS_NPs, paclitaxel–cholesterol complex-loaded lecithin–chitosan nanoparticles.

that of PEI.[56] So such behavior of PTX-CH-loaded LCS_NPs contributed to the increased intracellular drug release when the LCS_NPs were trapped in endosomal compartments with acidic environment.[57] All these might help to shed light on improved antitumor efficacy of PTX-CH-loaded LCS_NPs in vivo.

4T1 cells can metastasize even at an early stage, primarily to the lung and liver.[58,59] The lungs and livers isolated from normal and tumor-bearing mice were fixed and stained with H&E. The results of histopathological examination are demonstrated in Figure 11. In the saline and blank LCS_NPs group, large areas of the metastatic region were observed in the lungs and livers (red circles and arrows) instead of

normal physiological structures, which suggested significant tumor micrometastasis in these two groups. But there was no distinguishable tumor micrometastasis in slices of lungs in PTX-CH-loaded LCS_NPs group, and the number of metastatic regions was much smaller than that of PTX group. The results of H&E suggested that PTX-CH-loaded LCS_NPs showed better ability to inhibit tumor metastasis than PTX by intratumoral injection.

Survival analysis

Given the improved antitumor efficacy of PTX-CH-loaded LCS_NPs by intratumoral injection, the evaluation of the effect on survival rates was also investigated (Figure 12).
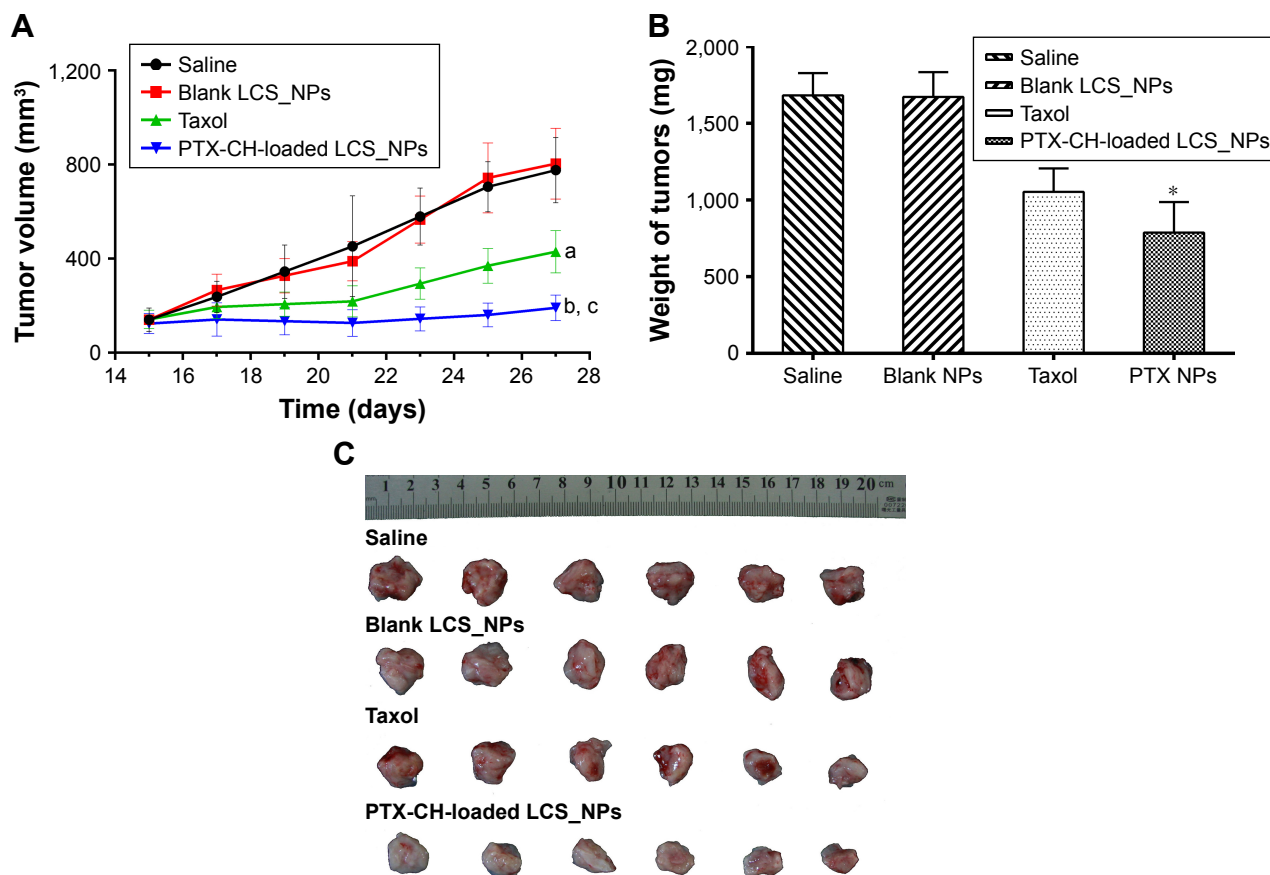
Figure 9 Studies of antitumor efficacy of PTX-CH-loaded LCS_NPs in vivo.
Notes: (**A**) Tumor volume of mice treated with saline, blank LCS_NPs, PTX, PTX-CH-loaded LCS_NPs (mean ± SD, n=6). a, $P<0.001$; b, $P<0.001$ vs saline; c, $P<0.001$ vs PTX. (**B**) Weight of isolated tumors in groups of saline, blank LCS_NPs, PTX, PTX-CH-loaded LCS_NPs (mean ± SD, n=6). *$P<0.05$ vs PTX. (**C**) Isolated tumor tissues of mice treated with saline, blank LCS_NPs, PTX, PTX-CH-loaded LCS_NPs.
Abbreviations: LCS_NPs, lecithin–chitosan nanoparticles; PTX-CH-loaded LCS_NPs, paclitaxel–cholesterol complex-loaded lecithin–chitosan nanoparticles.
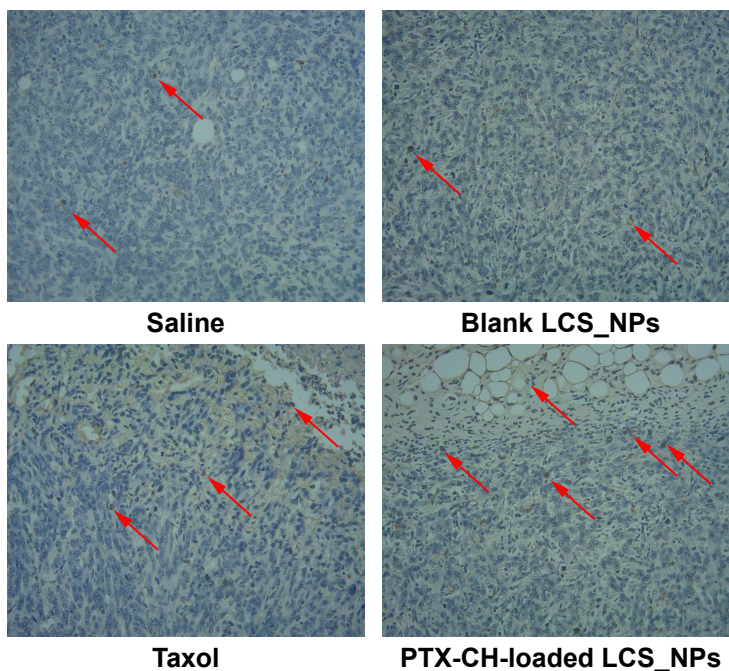
Figure 10 TUNEL assay of tumor tissues isolated from mice treated with saline, blank LCS_NPs, PTX, PTX-CH-loaded LCS_NPs, and observed by optical microscope, 100×. Red arrows represent apoptotic tumor cells.
Abbreviations: LCS_NPs, lecithin–chitosan nanoparticles; PTX-CH-loaded LCS_NPs, paclitaxel–cholesterol complex-loaded lecithin–chitosan nanoparticles.
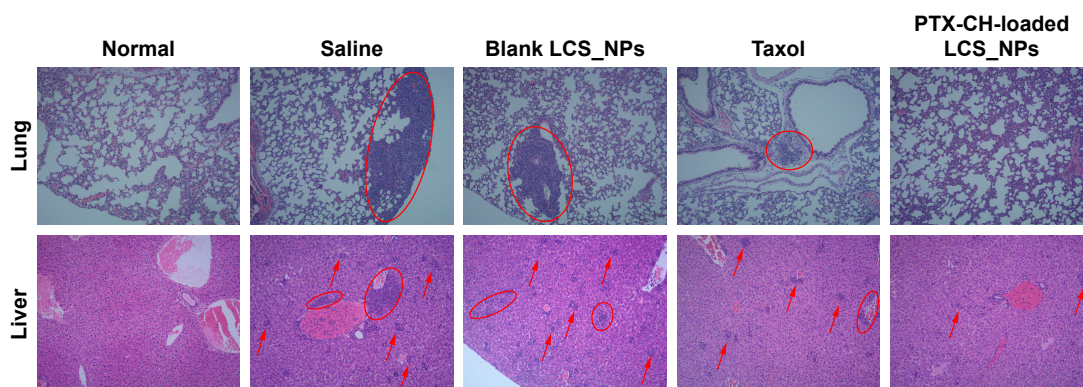
Figure 11 Lungs and livers of normal and tumor-bearing mice treated with saline, blank LCS_NPs, PTX, PTX-CH-loaded LCS_NPs were stained with H&E and observed by optical microscope, 100×. Normal lungs and livers were taken as a comparison; circled areas and red arrows show the metastatic areas.
Abbreviations: LCS_NPs, lecithin–chitosan nanoparticles; PTX-CH-loaded LCS_NPs, paclitaxel–cholesterol complex-loaded lecithin–chitosan nanoparticles.

All the mice in the saline and blank LCS_NPs groups died within 38 days. Meanwhile, the average survival time of PTX-CH-loaded LCS_NPs group was significantly prolonged to 56 days, demonstrating that the survival time of tumor-bearing mice could be effectively prolonged by intratumoral injection PTX-CH-loaded LCS_NPs.

Conclusion

In this study, we have successfully prepared PTX-CH-loaded LCS_NPs for palliative intratumoral injection therapy and evaluated the antitumor efficacy in vitro and in vivo. The results indicated that drug delivery of PTX-CH-loaded LCS_NPs into tumor cells was more efficient, due to their pH-sensitive PTX release pattern and highly efficient endocytosis. Also, PTX-CH-loaded LCS_NPs had a more significant effect on cell proliferation and apoptosis in vitro. Importantly, PTX-CH-loaded LCS_NPs effectively inhibited growth and metastasis of tumors, and prolonged the average survival time of tumor-bearing mice. PTX-CH-loaded LCS_NPs provided an alternative therapy in the field of palliative chemotherapy by intratumoral injection. Future study will focus on individualized treatment of tumors and the antitumor effect of PTX-CH-loaded LCS_NPs on other solid carcinomas, such as squamous cell carcinoma.

Acknowledgments

Disclosure

The authors report no conflicts of interest in this work.

Figure 12 Curve of survival ratio of 4T1 tumor-bearing mice intratumorally injected with saline, blank LCS_NPs, PTX, PTX-CH-loaded LCS_NPs, respectively (n=10).
Abbreviations: LCS_NPs, lecithin–chitosan nanoparticles; PTX-CH-loaded LCS_NPs, paclitaxel–cholesterol complex-loaded lecithin–chitosan nanoparticles.

References

1. Müller JM, Erasmi H, Stelzner M, Zieren U, Pichlmaier H. Surgical therapy of oesophageal carcinoma. *Br J Surg*. 1990;77(8):845–857.
2. Allen AM, Rabin MS, Reilly JJ, Mentzer SJ. Unresectable adenoid cystic carcinoma of the trachea treated with chemoradiation. *J Clin Oncol*. 2007;25(34):5521–5523.
3. Bruix J, Sherman M. Practice Guidelines Committee AAftSoLD. Management of hepatocellular carcinoma. *Hepatology*. 2005;42(5):1208–1236.
4. Shapiro MJ. Management of malignant biliary obstruction: nonoperative and palliative techniques. *Oncology*. 1995;9(6):493–496.
5. Bakker RC, van Es RJJ, Rosenberg AJWP, et al. Intratumoral injection of radioactive holmium-166 microspheres in recurrent head and neck squamous cell carcinoma. *Nucl Med Commun*. 2018;39(3):1–221.
6. Mehta HJ, Begnaud A, Penley AM, et al. Treatment of isolated mediastinal and hilar recurrence of lung cancer with bronchoscopic endobronchial ultrasound guided intratumoral injection of chemotherapy with cisplatin. *Lung Cancer*. 2015;90(3):542–547.
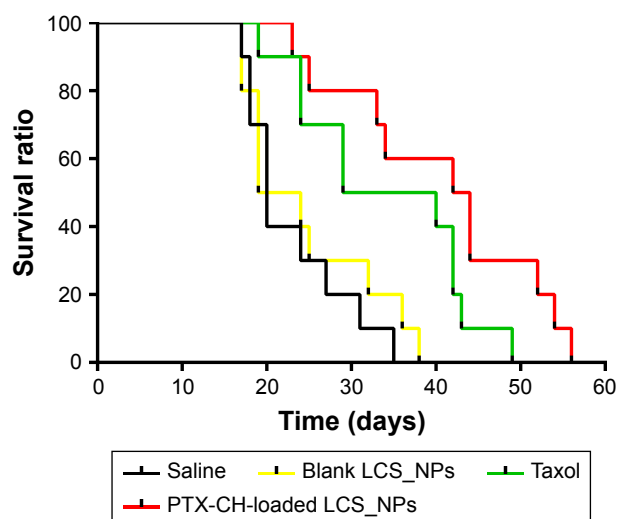
7. Mehta HJ, Jantz MA. Endobronchial ultrasound-guided intratumoral injection of cisplatin for the treatment of isolated mediastinal recurrence of lung cancer. *J Vis Exp*. 2017;(120).

8. Li SY, Li Q, Guan WJ, et al. Effects of para-toluenesulfonamide intratumoral injection on non-small cell lung carcinoma with severe central airway obstruction: a multi-center, non-randomized, single-arm, open-label trial. *Lung Cancer*. 2016;98:43–50.

9. Gimbel MI, Delman KA, Zager JS. Therapy for unresectable recurrent and in-transit extremity melanoma. *Cancer Control*. 2008;15(3):225–232.

10. Ramakrishnaiah VP, Ramkumar J, Pai D. Intratumoural injection of absolute alcohol in carcinoma of gastroesophageal junction for palliation of dysphagia. *Ecancermedicalscience*. 2014;8:395.

11. Park SW, Lee DH, Park YS, Chung JB, Kang JK, Song SY. Percutaneous transhepatic choledochoscopic injection of ethanol with OK-432 mixture for palliation of malignant biliary obstruction. *Gastrointest Endosc*. 2003;57(6):769–773.

12. Burris HA, Vogel CL, Castro D, et al. Intratumoral cisplatin/epinephrine-injectable gel as a palliative treatment for accessible solid tumors: a multicenter pilot study. *Otolaryngol Head Neck Surg*. 1998;118(4):496–503.

13. Xie M, Zhou L, Hu T, Yao M. Intratumoral delivery of paclitaxel-loaded poly(lactic-co-glycolic acid) microspheres for Hep-2 laryngeal squamous cell carcinoma xenografts. *Anticancer Drugs*. 2007;18(4):459–466.

14. Duncan IC, Fourie PA, Alberts AS. Direct percutaneous intratumoral bleomycin injection for palliative treatment of impending quadriplegia. *Am J Neuroradiol*. 2004;25(6):1121–1123.

15. Zhao L, Zhu L, Liu F, et al. pH triggered injectable amphiphilic hydrogel containing doxorubicin and paclitaxel. *Int J Pharm*. 2011;410(1–2):83–91.

16. Bragta P, Sidhu RK, Jyoti K, et al. Intratumoral administration of carboplatin bearing poly (ε-caprolactone) nanoparticles amalgamated with in situ gel tendered augmented drug delivery, cytotoxicity, and apoptosis in melanoma tumor. *Colloids Surf B Biointerfaces*. 2018;166:339–348.

17. Jiang Y, Meng X, Wu Z, Qi X. Modified chitosan thermosensitive hydrogel enables sustained and efficient anti-tumor therapy via intratumoral injection. *Carbohydr Polym*. 2016;144:245–253.

18. Al-Abd AM, Hong KY, Song SC, Kuh HJ. Pharmacokinetics of doxorubicin after intratumoral injection using a thermosensitive hydrogel in tumor-bearing mice. *J Control Release*. 2010;142(1):101–107.

19. Lin WY, Tsai SC, Hsieh JF, Wang SJ. Effects of 90Y-microspheres on liver tumors: comparison of intratumoral injection method and intra-arterial injection method. *J Nucl Med*. 2000;41(11):1892–1897.

20. Chang G, Li C, Lu W, Ding J. N-Boc-histidine-capped PLGA-PEG-PLGA as a smart polymer for drug delivery sensitive to tumor extracellular pH. *Macromol Biosci*. 2010;10(10):1248–1256.

21. Xu X, Chen X, Wang Z, Jing X. Ultrafine PEG-PLA fibers loaded with both paclitaxel and doxorubicin hydrochloride and their in vitro cytotoxicity. *Eur J Pharm Biopharm*. 2009;72(1):18–25.

22. Greish K. Enhanced permeability and retention (EPR) effect for anticancer nanomedicine drug targeting. *Methods Mol Biol*. 2010;624:25–37.

23. Wu X, Landfester K, Musyanovych A, Guy RH. Disposition of charged nanoparticles after their topical application to the skin. *Skin Pharmacol Physiol*. 2010;23(3):117–123.

24. Tan Q, Liu W, Guo C, Zhai G. Preparation and evaluation of quercetin-loaded lecithin-chitosan nanoparticles for topical delivery. *Int J Nanomed*. 2011;6:1621–1630.

25. Sonvico F, Cagnani A, Rossi A, et al. Formation of self-organized nanoparticles by lecithin/chitosan ionic interaction. *Int J Pharm*. 2006;324(1):67–73.

26. Wike-Hooley JL, Haveman J, Reinhold HS. The relevance of tumour pH to the treatment of malignant disease. *Radiother Oncol*. 1984;2(4):343–366.

27. Nam JP, Park SC, Kim TH, et al. Encapsulation of paclitaxel into lauric acid-O-carboxymethyl chitosan-transferrin micelles for hydrophobic drug delivery and site-specific targeted delivery. *Int J Pharm*. 2013;457(1):124–135.

28. Pan Z, Gao Y, Heng L, et al. Amphiphilic N-(2,3-dihydroxypropyl)-chitosan-cholic acid micelles for paclitaxel delivery. *Carbohydr Polym*. 2013;94(1):394–399.

29. Rowinsky EK, Donehower RC. Paclitaxel (Taxol). *N Engl J Med*. 1995;332(15):1004–1014.

30. Xu J, Ma L, Liu Y, Xu F, Nie J, Ma G. Design and characterization of antitumor drug paclitaxel-loaded chitosan nanoparticles by W/O emulsions. *Int J Biol Macromol*. 2012;50(2):438–443.

31. Tao Y, Xu J, Chen M, Bai H, Liu X. Core cross-linked hyaluronan-styrylpyridinium micelles as a novel carrier for paclitaxel. *Carbohydrate Polym*. 2012;88(1):118–124.

32. Sparreboom A, Scripture CD, Trieu V, et al. Comparative preclinical and clinical pharmacokinetics of a cremophor-free, nanoparticle albumin-bound paclitaxel (ABI-007) and paclitaxel formulated in Cremophor (Taxol). *Clin Cancer Res*. 2005;11(11):4136–4143.

33. Xia XJ, Guo RF, Liu YL, et al. Formulation, characterization and hypersensitivity evaluation of an intravenous emulsion loaded with a paclitaxel-cholesterol complex. *Chem Pharm Bull*. 2011;59(3):321–326.

34. Liu Y, Liu L, Zhou C, Xia X. Self-assembled lecithin/chitosan nanoparticles for oral insulin delivery: preparation and functional evaluation. *Int J Nanomedicine*. 2016;11:761–769.

35. Singh B, Mehta G, Kumar R, Bhatia A, Ahuja N, Katare OP. Design, development and optimization of nimesulide-loaded liposomal systems for topical application. *Curr Drug Deliv*. 2005;2(2):143–153.

36. Lv Q, Yu A, Xi Y, et al. Development and evaluation of penciclovir-loaded solid lipid nanoparticles for topical delivery. *Int J Pharm*. 2009;372(1–2):191–198.

37. Huh KM, Lee SC, Cho YW, Lee J, Jeong JH, Park K. Hydrotropic polymer micelle system for delivery of paclitaxel. *J Control Release*. 2005;101(1–3):59–68.

38. Jin M, Jin G, Kang L, Chen L, Gao Z, Huang W. Smart polymeric nanoparticles with pH-responsive and PEG-detachable properties for co-delivering paclitaxel and survivin siRNA to enhance antitumor outcomes. *Int J Nanomedicine*. 2018;13:2405–2426.

39. Stevens PJ, Sekido M, Lee RJ. A folate receptor-targeted lipid nanoparticle formulation for a lipophilic paclitaxel prodrug. *Pharm Res*. 2004;21(12):2153–2157.

40. Ye J, Liu Y, Xia X, et al. Improved safety and efficacy of a lipid emulsion loaded with a paclitaxel-cholesterol complex for the treatment of breast tumors. *Oncol Rep*. 2016;36(1):399–409.

41. Senyiğit T, Sonvico F, Barbieri S, Ozer O, Santi P, Colombo P. Lecithin/chitosan nanoparticles of clobetasol-17-propionate capable of accumulation in pig skin. *J Control Release*. 2010;142(3):368–373.

42. Fakhry A, Schneider GB, Zaharias R, Şenel S. Chitosan supports the initial attachment and spreading of osteoblasts preferentially over fibroblasts. *Biomaterials*. 2004;25(11):2075–2079.

43. Weiszhár Z, Czúcz J, Révész C, Rosivall L, Szebeni J, Rozsnyay Z. Complement activation by polyethoxylated pharmaceutical surfactants: Cremophor-EL, Tween-80 and Tween-20. *Eur J Pharm Sci*. 2012;45(4):492–498.

44. Witz IP, Levy-Nissenbaum O. The tumor microenvironment in the post-PAGET era. *Cancer Lett*. 2006;242(1):1–10.

45. Weber CE, Kuo PC. The tumor microenvironment. *Surg Oncol*. 2012;21(3):172–177.

46. Khalil IA, Kogure K, Akita H, Harashima H. Uptake pathways and subsequent intracellular trafficking in nonviral gene delivery. *Pharmacol Rev*. 2006;58(1):32–45.

47. Wang LH, Rothberg KG, Anderson RG. Mis-assembly of clathrin lattices on endosomes reveals a regulatory switch for coated pit formation. *J Cell Biol*. 1993;123(5):1107–1117.

48. Liu J, Shapiro JI. Endocytosis and signal transduction: basic science update. *Biol Res Nurs*. 2003;5(2):117–128.

49. Lamaze C, Schmid SL. The emergence of clathrin-independent pinocytic pathways. *Curr Opin Cell Biol*. 1995;7(4):573–580.

50. Nam HY, Kwon SM, Chung H, et al. Cellular uptake mechanism and intracellular fate of hydrophobically modified glycol chitosan nanoparticles. *J Control Release*. 2009;135(3):259–267.

51. Chiu YL, Ho YC, Chen YM, et al. The characteristics, cellular uptake and intracellular trafficking of nanoparticles made of hydrophobically-modified chitosan. *J Control Release*. 2010;146(1):152–159.

52. Meng H, Yang S, Li Z, et al. Aspect ratio determines the quantity of mesoporous silica nanoparticle uptake by a small GTPase-dependent macropinocytosis mechanism. *ACS Nano*. 2011;5(6):4434–4447.

53. Manunta M, Tan PH, Sagoo P, Kashefi K, George AJ. Gene delivery by dendrimers operates via a cholesterol dependent pathway. *Nucleic Acids Res*. 2004;32(9):2730–2739.

54. Jiang S, Rhee SW, Gleeson PA, Storrie B. Capacity of the Golgi apparatus for cargo transport prior to complete assembly. *Mol Biol Cell*. 2006;17(9):4105–4117.

55. Trielli MO, Andreassen PR, Lacroix FB, Margolis RL. Differential Taxol-dependent arrest of transformed and nontransformed cells in the G1 phase of the cell cycle, and specific-related mortality of transformed cells. *J Cell Biol*. 1996;135(3):689–700.

56. Richard I, Thibault M, de Crescenzo G, Buschmann MD, Lavertu M. Ionization behavior of chitosan and chitosan–DNA polyplexes indicate that chitosan has a similar capability to induce a proton-sponge effect as PEI. *Biomacromolecules*. 2013;14(6):1732–1740.

57. Cao N, Cheng D, Zou S, Ai H, Gao J, Shuai X. The synergistic effect of hierarchical assemblies of siRNA and chemotherapeutic drugs co-delivered into hepatic cancer cells. *Biomaterials*. 2011;32(8): 2222–2232.

58. Kaur P, Nagaraja GM, Zheng H, et al. A mouse model for triple-negative breast cancer tumor-initiating cells (TNBC-TICs) exhibits similar aggressive phenotype to the human disease. *BMC Cancer*. 2012; 12(1):120.

59. Subramanian A, Manigandan A, Sivashankari PR, Sethuraman S. Development of nanotheranostics against metastatic breast cancer – a focus on the biology & mechanistic approaches. *Biotechnol Adv*. 2015;33(8): 1897–1911.